



## OPEN ACCESS

## EDITED BY

Chunlong Li,  
Huazhong Agricultural University, China

## REVIEWED BY

Tao Qin,  
Northwest A&F University, China  
Liru Dou,  
China Agricultural University, China

## \*CORRESPONDENCE

Na Lian  
✉ lianna@bjfu.edu.cn

<sup>†</sup>These authors have contributed equally to this work

## SPECIALTY SECTION

This article was submitted to  
Plant Metabolism and Chemodiversity,  
a section of the journal  
Frontiers in Plant Science

RECEIVED 05 February 2023

ACCEPTED 22 February 2023

PUBLISHED 13 March 2023

## CITATION

Qi M, Wang S, Li N, Li L, Zhang Y,  
Xue J, Wang J, Wu R and Lian N  
(2023) Genome-wide analysis of  
*TPX2* gene family in *Populus trichocarpa*  
and its specific response genes under  
various abiotic stresses.  
*Front. Plant Sci.* 14:1159181.  
doi: 10.3389/fpls.2023.1159181

## COPYRIGHT

© 2023 Qi, Wang, Li, Li, Zhang, Xue, Wang,  
Wu and Lian. This is an open-access article  
distributed under the terms of the [Creative  
Commons Attribution License \(CC BY\)](#). The  
use, distribution or reproduction in other  
forums is permitted, provided the original  
author(s) and the copyright owner(s) are  
credited and that the original publication in  
this journal is cited, in accordance with  
accepted academic practice. No use,  
distribution or reproduction is permitted  
which does not comply with these terms.

# Genome-wide analysis of *TPX2* gene family in *Populus trichocarpa* and its specific response genes under various abiotic stresses

Meng Qi<sup>1†</sup>, Shengjie Wang<sup>1†</sup>, Na Li<sup>1†</sup>, Lingfeng Li<sup>1</sup>, Yue Zhang<sup>1</sup>,  
Jingyi Xue<sup>1</sup>, Jingyi Wang<sup>1</sup>, Rongling Wu<sup>1</sup> and Na Lian<sup>1,2\*</sup>

<sup>1</sup>State Key Laboratory of Tree Genetics and Breeding, College of Biological Sciences and Technology, Beijing Forestry University, Beijing, China, <sup>2</sup>National Engineering Research Center of Tree Breeding and Ecological Restoration, Beijing Forestry University, Beijing, China

Microtubules are essential for regulating cell morphogenesis, plant growth, and the response of plants to abiotic stresses. *TPX2* proteins are the main players determining the spatiotemporally dynamic nature of the MTs. However, how *TPX2* members respond to abiotic stresses in poplar remains largely unknown. Herein, 19 *TPX2* family members were identified from the poplar genome and analyzed the structural characteristics as well as gene expression patterns. All *TPX2* members had the conserved structural characteristics, but exhibited different expression profiles in different tissues, indicating their varying roles during plant growth. Additionally, several light, hormone, and abiotic stress responsive *cis*-acting regulatory elements were detected on the promoters of *PtTPX2* genes. Furthermore, expression analysis in various tissues of *Populus trichocarpa* showed that the *PtTPX2* genes responded differently to heat, drought and salt stress. In summary, these results provide a comprehensive analysis for the *TPX2* gene family in poplar and an effective contribution to revealing the mechanisms of *PtTPX2* in the regulatory network of abiotic stress.

## KEYWORDS

*Populus*, gene expression pattern, gene structure, phase separation, stress treatment, *PtTPX2* gene family

## 1 Introduction

Microtubules (MTs) are hollow tubular structures polymerized by the  $\alpha$ -tubulin and  $\beta$ -tubulin heterodimers that play critical roles in cell division, cell expansion and morphogenesis during plant growth and cell morphogenesis (Fletcher and Mullins, 2010; Ren et al., 2017). The functions and dynamics of MTs depend on multiple microtubule-associated proteins (MAPs) and other regulators, such as  $\gamma$ -tubulin complex ( $\gamma$ -TuC), microtubule bundling proteins and microtubule destabilizing proteins (Lloyd,

2011; Hamada, 2014). It has been reported that MTs can rapidly alter their organization in response to various environmental signals, such as light, low temperatures and salt stress (Chen et al., 2016; Lian et al., 2021). For instance, salt stress induces the rapid depolymerization of MTs, followed by the reassembly of new microtubule networks, which is vital for plant survival under high-salinity environment (Wang et al., 2011; Wang and Mao, 2019). Furthermore, several MAPs have been implicated in these processes. For example, the degradation of SPIRAL1, a microtubule-stabilizing protein, is required for the salinity-induced rapid depolymerization of MTs and for plant salt-stress tolerance (Wang et al., 2011).

Targeting Protein for Xklp2 (TPX2) contains a highly conserved TPX2 domain (Pfam: PF06886) and acts as a microtubule-binding protein to regulate the stability and organization of cortical MTs in animals and plants (Wittmann et al., 2000; Brunet et al., 2004; Vos et al., 2008). TPX2 family proteins contain TPX2, TPX2-importin, TPX2-C<sup>KLEEK</sup> and WAVE-DAMPENED2-like New Domain (WAND). TPX2\_importin domain mediates the localization of Xklp2 to the mitotic spindle. The TPX2-C domain, a highly conserved and kinesin-interacting domain, is located on the very C-terminus. Plant TPXL binds and activates Aurora 1 through the conserved Aurora-binding domain on the N-terminus, and Aurora 1 phosphorylates TPX2 independently of the binding domain (Smertenko et al., 2021). In addition, WAND, a class of conservative domain, is also discovered. Furthermore, the *Xenopus* TPX2 protein undergoes phase separation to form droplets with tubulin, which is essential for microtubule nucleation. The disordered N-terminal region of TPX2 enhances the phase separation and efficiency of MTs nucleation (King and Petry, 2020; Safari et al., 2021).

In the past two decades, several TPX2 proteins have been reported in various plants during growth and development, such as TPX2, MAP20, WVD2 and WDL (Perrin et al., 2007; Rajangam et al., 2008; Liu et al., 2013; Sun et al., 2015; Lian et al., 2017; Smertenko et al., 2020). The *Arabidopsis thaliana* WVD2 (AtWVD2) promotes MTs bundling to improve their stability, which plays a critical role in polar cell elongation (Perrin et al., 2007). AtWDL3 stabilizes MTs and functions in hypocotyl cell elongation in response to light, while the protein is degraded under dark conditions (Liu et al., 2013; Lian et al., 2017). AtWDL5 stabilizes MTs to promote ethylene-associated MTs reassembly (Sun et al., 2015). *Populus tremula* × *tremuloides* MAP20 (PttMAP20) stabilizes MTs and acts as a target of the cell wall synthesis herbicide 2,6-dichlorobenzonitrile, playing an important role in cell wall biosynthesis (Rajangam et al., 2008). The *Brachypodium distachyon* MAP20 (BdMAP20) suppresses MTs depolymerization and functions in metaxylem pit development (Smertenko et al., 2020). Furthermore, TPX2 proteins are also involved in various abiotic stress responses in plants (Dou et al., 2018; Smertenko et al., 2020). AtWDL5 is involved in ethylene-mediated MTs reassembly in response to salt stress (Dou et al., 2018). BdMAP20 is involved in the regulation of vascular bundle development and contributes to drought recovery (Smertenko et al., 2020).

Poplar is an economically and ecologically important perennial woody plant that is widely cultivated. It is seriously affected by various environmental stresses such as soil salinization, heat and

drought (Zhang et al., 2019). Poplar also serves as a model for elucidating physiological and molecular mechanisms of development and stress tolerance in tree species based on its rapid growth characteristics (Wu et al., 2021). Research has shown that MAPs are key regulatory molecules participating in plant growth and responses to environmental signals. At present, most studies on TPX2 proteins in abiotic stress still focus on model plants, such as *Arabidopsis*. In poplars, the family members of TPX2 and their regulatory mechanisms in response to abiotic stress are largely unknown. In this study, *Populus trichocarpa* TPX2 (*PtTPX2*) genes were systematically and comprehensively analyzed. Specifically, analyses of phylogenetic relationships, protein physicochemical properties, gene structures, protein domain, chromosome distributions, intrinsically disordered protein regions, promoter *cis*-acting elements of *PtTPX2* genes and collinearity analysis of species were performed. RT-qPCR showed that *PtTPX2* genes have different expression patterns in poplar. By analyzing the results of RT-qPCR, it was found that *PtWDL6* was up-regulated in response to salt, heat and drought treatments. These findings indicate that *PtWDL6* plays an important role in the resistance to abiotic stresses. Therefore, we cloned the *PtWDL6* gene and found that *PtWDL6* can bind MTs through subcellular localization analysis. These results suggest that *PtWDL6* may be involved in poplar response to abiotic stress by regulating MTs. Collectively, this study performs an initial characterization of the structures and functions of the *PtTPX2* family, extends the relationship between the plant TPX2 family and abiotic stress tolerance and establishes a foundation for future studies on the role of TPX2 genes in stress tolerance.

## 2 Materials and methods

### 2.1 Plant materials and treatments

One-month-old *Populus alba* × *Populus glandulosa* (84K) seedlings were cultivated on sterile WPM at 25°C with 16 h of light of 5,000 lx and 8 h of dark. For salt stress, one-month-old seedlings were transferred from initial solid WPM medium (without NaCl) to liquid WPM media supplemented with 200 mM NaCl for 24 hours (Xu et al., 2018). For heat stress, one-month-old seedlings were transferred to 42 °C for 24 h. For drought stress, one-month-old seedlings were transferred to a medium containing 200 mM mannitol (simulated drought) for 24 h. Controls for the above treatments were incubated without any treatment. After treatment, various tissues were harvested from three plants of each treatment in different times. All samples obtained were frozen in liquid nitrogen and rapidly stored at -80°C for subsequent experiments.

### 2.2 Identification and phylogenetic analysis of TPX2 genes in *Populus trichocarpa*

To identify putative TPX2 genes in *Populus trichocarpa*, the protein sequence of *Arabidopsis thaliana* TPX2 genes were obtained

from TAIR (<https://www.arabidopsis.org/>, accessed on 20 October 2022) and used as the query sequences to screen all the candidate proteins in *Populus trichocarpa* with the BLASTp search (<https://phytozome-next.jgi.doe.gov/>, accessed on 20 October 2022) (Luo et al., 2022). In order to ensure the accuracy and comprehensiveness of the sequences, the Pfam number (PF06886) and HMM model files of the TPX2 conserved domain were searched through the PFAM database (<http://pfam.xfam.org/>, accessed on 20 October 2022), and the TPX2 family genes were screened by the HMM model file on the HMMER website (<http://hmmer.org/>, accessed on 20 October 2022) (Cao et al., 2020).

The amino acid sequences of TPX2 proteins from *Arabidopsis thaliana*, *Populus trichocarpa*, *Gossypium hirsutum* and *Eucalyptus grandis* were obtained from TAIR (<https://www.arabidopsis.org/>, accessed on 25 December 2022) and Phytozome (<https://phytozome-next.jgi.doe.gov/>, accessed on 25 December 2022). These TPX2 sequences were aligned using the ClustalW program (Chenna et al., 2003). The parameters were set by default. A neighbor-joining (NJ) phylogenetic tree was constructed using the MEGA7.0.26 program with 1000 bootstrap replicates (Lei et al., 2019).

### 2.3 Characteristic analysis of PtTPX2

The length of the coding sequences and number of amino acids were calculated by using the TBtools software (Chen et al., 2020). The molecular weight and isoelectric point of PtTPX2 proteins were analyzed by using the ExPASy ProtParam tool (<https://web.expasy.org/protparam/>, accessed on 20 October 2022) (Tuskan et al., 2006). The conserved motifs of PtTPX2 proteins were predicted by the online website MEME (<http://meme-suite.org/index.html/>, accessed on 20 October 2022) (Bailey and Gribskov, 1998). To further visualize the motifs' compositions and protein structures, integration analysis was conducted using TBtools software. Based on the General Feature Format (GFF) information from the Phytozome database, the chromosomal distribution of the *PtTPX2* genes was confirmed and visualized by using Mapchart software (Voorrips, 2002). The promoter sequences 2000 bp upstream of the *Populus trichocarpa* TPX2 genes were extracted from the Phytozome database. The prediction of *cis*-acting elements of the promoter region was identified using the PlantCare database (<http://bioinformatics.psb.ugent.be/webtools/plantcare/html/>, accessed on 20 October 2022) (Lescot et al., 2002).

### 2.4 Chromosomal distribution and collinear analysis of PtTPX2

The chromosomal positions of genes were mapped using the TBtools software (Chen et al., 2020) based on annotated files of genomic structural information of *Arabidopsis thaliana*, *Populus trichocarpa*, *Gossypium hirsutum* and *Eucalyptus grandis*. These genomic data were obtained from Phytozome ([\[next.jgi.doe.gov/\]\(https://phytozome-next.jgi.doe.gov/\), accessed on 25 January 2023\). TBtools software was used to visualize intraspecific and interspecific collinearity of \*Populus trichocarpa\*. Advanced Circos function from TBtools software was used for visualization within \*Populus trichocarpa\* species. Multiple Synteny Plot function from TBtools software was used to visualize collinearity of \*Populus trichocarpa\* and \*Arabidopsis thaliana\*, \*Populus trichocarpa\* and \*Gossypium hirsutum\*, \*Populus trichocarpa\* and \*Eucalyptus grandis\*.](https://phytozome-</a></p>
</div>
<div data-bbox=)

### 2.5 Prediction of PtTPX2 proteins' intrinsically disordered regions

Intrinsically disordered regions (IDRs) are protein regions characterized by lack of definite structures. IDRs of all PtTPX2 proteins were predicted by using the online PONDR program (<http://www.pondr.com/>, accessed on 25 January 2023) (Xue et al., 2010). The presence of IDRs makes it easier for proteins to form droplet shape, inducing phase transition generation and regulation.

### 2.6 Total RNA extraction and cDNA reverse transcription synthesis

Total RNA was extracted using the Eastep Super Total RNA Extraction Kit (LS1040, Shanghai Promega, Shanghai, China). The quality of RNA samples were determined by the NanoDrop 8000 (Thermo Fisher Scientific, Waltham, Massachusetts, USA) (Desjardins and Conklin, 2010; Lei et al., 2019). Then, using 1 µg RNA as the template, the RNA was reverse transcribed into cDNA using the rapid quantitative RT Supermix Kit (M-MLV Reverse Transcriptase, Mi Si Century Biotechnology company, Shanghai, China) (Qi et al., 2022). The cDNA was stored at -20 °C for subsequent RT-qPCR experiments.

### 2.7 PCR primer design and real-time quantitative PCR analysis

Specific RT-qPCR primers were designed using Primer 3 plus software (<https://www.primer3plus.com/index.html/>, accessed on 1 August 2022), and then the best primers for specificity were selected (Supplementary Table S1). The number of primer bases was between 18 and 20 bp, and the sequence length was between 80 and 120 bp. Poplar 18S rRNA was used as a reference gene to normalize the expression data. RT-qPCR was detected by CFX connect in a 10 µl per well system. Calculations were performed using the  $2^{-\Delta\Delta C_t}$  method with a *t*-test to analyze significant differences (Meng et al., 2016). Three biological replicates were set up for each sample and three technical replicates for each biological replicate. Microsoft Excel software was used for data analysis, Graphpad prism9 and TBtools software was used for drawing.

## 2.8 Subcellular localization of PtWDL6 protein

The amplified CDS of *PtWDL6* and the sequence of expressing green fluorescent protein (GFP) were inserted into the plasmid vector (pCAMBIA1390) by homologous recombination. Subcellular localization of PtWDL6 and cortical MTs was visualized using transiently expressed *UBQ : PtWDL6-GFP* and *UBQ : MBD-mCherry* constructs expressed in tobacco leaf epidermal cells (Liu et al., 2013; Dou et al., 2021). The plasmid was transformed into *Agrobacterium tumefaciens* GV3101, and the two vectors were transiently co-expressed in tobacco epidermal cells. All fluorescence signals of the samples were detected using a confocal laser scanning microscope system (Zeiss LSM 810).

## 3 Results

### 3.1 Characterization and phylogenetic analysis of PtTPX2 genes

In this study, we screened the *TPX2* genes from the *Populus trichocarpa* v4.1 (<https://phytozome-next.jgi.doe.gov>, accessed on

21 October 2022), named as *PtMAP20*, *PtMAP20L*, *PtTPX2* and *PtWDL*. Detailed characteristics and information of these genes were analyzed and summarized in Table 1, including the molecular weight (Mw), the isoelectric point (PI) and the number of amino acids (AAs). In this family, the proteins ranged from 177 (*PtMAP20*) to 817 (*PtTPX2-1*) amino acids in length. The predicted molecular weight varied from 20.79 kDa (*PtMAP20*) to 92.33 kDa (*PtTPX2-1*). Except for *PtWDL10*, the number of predicted isoelectric points was more than seven, indicating that *PtTPX2* proteins are rich in basic amino acids. Amino acid composition analysis showed that the proportion of amino acid composition of *PtTPX2* proteins were similar. The proportion of the charged amino acids was 36.01% to 45.63%. The proportion of the acidic amino acids was between 12.57% and 17.48%, and the proportion of basic amino acids was between 18.79% and 23.07%. The proportion of polar amino acids ranged from 22.72% to 32.61%, and the proportion of hydrophobic amino acids ranged from 20.6% to 26.83%.

To investigate the evolutionary relationships and potential functional characteristics of the *PtTPX2* family members, a phylogenetic tree was constructed using all the *TPX2* full-length protein sequences from *Populus trichocarpa*, *Eucalyptus grandis*, *Gossypium hirsutum* and *Arabidopsis thaliana* (Supplementary

TABLE 1 Information of PtTPX2 protein structures and amino acid ratios.

Amino acid (s)	Gene ID	Mw	PI	AAs	Number count (% by weight)				
					Charged	Acidic	Basic	Polar	Hydrophobic
					(R K H Y C D E)	(D E)	(K R)	(N C Q S T Y)	(A I L F W V)
PtMAP20	Potri.017G144061	20794.00	9.70	177	70.00	21.00	33.00	41.00	49.00
PtMAP20L1	Potri.004G118700	61765.51	9.29	540	45.46	16.99	23.07	26.13	22.53
PtMAP20L2	Potri.017G092100	61279.02	9.18	536	45.45	16.47	22.33	27.14	21.75
PtTPX2-1	Potri.007G138600	92337.81	9.41	817	40.23	14.71	20.22	25.97	24.12
PtTPX2-2	Potri.017G013100	91647.10	9.42	812	41.37	15.15	20.70	24.25	24.46
PtWDL1	Potri.005G055900	40115.68	9.74	365	44.66	13.82	22.48	28.33	20.60
PtWDL2	Potri.008G162800	43127.15	8.66	388	44.32	16.84	19.96	28.45	21.80
PtWDL3	Potri.010G076200	44295.84	8.42	405	42.55	16.11	18.79	26.28	23.44
PtWDL4	Potri.013G042800	39987.47	9.62	362	44.55	15.26	22.98	28.54	21.44
PtWDL5	Potri.006G200400	54009.10	9.71	504	36.01	12.94	19.65	32.06	21.37
PtWDL6	Potri.006G254400	48617.05	8.89	437	41.14	16.66	20.18	26.87	22.43
PtWDL7	Potri.016G066600	46904.30	9.04	504	36.51	13.25	19.42	32.61	21.40
PtWDL8	Potri.018G027500	46799.03	9.90	435	40.57	16.50	20.08	27.36	24.61
PtWDL9	Potri.001G336300	61199.83	9.46	548	39.52	13.89	19.94	28.86	23.80
PtWDL10	Potri.008G129300	71876.15	6.81	646	43.96	17.48	19.00	26.86	22.29
PtWDL11	Potri.008G180900	70957.03	9.55	648	38.47	14.08	20.11	30.82	24.18
PtWDL12	Potri.010G038100	59780.95	8.92	542	42.36	17.39	20.78	25.20	24.00
PtWDL13	Potri.010G053200	58901.13	9.52	534	39.11	13.58	19.44	27.38	26.83
PtWDL14	Potri.010G113000	72081.53	7.63	647	44.14	17.15	19.71	28.49	21.71

According to the properties of amino acids, they are classified as charged amino acids, acidic amino acids, basic amino acids and hydrophobic amino acids. Letters in brackets are amino acids for short.

Table S2). Based on the homology, the *PtTPX2* genes, together with other *TPX2* genes, were assigned to six different subclasses (Subclass I-VI) (Figure 1). Subclass VI contained the largest numbers of *TPX2* genes. Subclass I contained the smallest numbers of *TPX2* genes, including *AtMAP20*, *PtMAP20*, *EgMAP20* and two *GhMAP20* genes. In addition, we examined other evidence to support the reliability of this classification, such as gene structures, conserved motifs (Supplementary Figure S1).

### 3.2 Structural analysis of *PtTPX2* genes and proteins

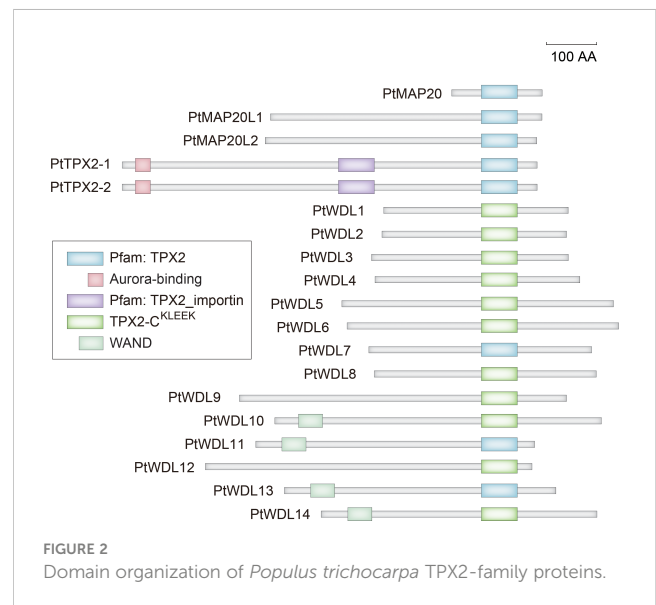
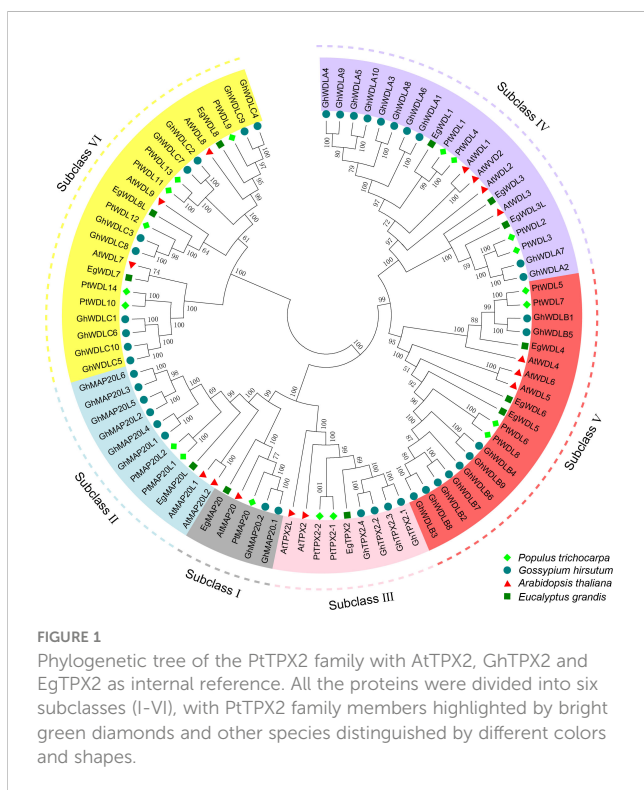
To further understand the structural diversity and similarity of *PtTPX2* genes and *PtTPX2* proteins, we analyzed the exon-intron structures, conserved motifs, and protein domains. Among 19 *PtTPX2* genes, genes grouped in the same subclass had similar gene structures (Supplementary Figure S1). The gene with the shortest length, *PtMAP20*, contained an extremely short first exon, and the six *PtWDL* (*PtWDL9*-*PtWDL14*) members also contained a short first exon. However, the subclass II members *PtMAP20L1* and *PtMAP20L2* contained a relatively long first exon among all *PtTPX2* genes. The two genes with the longest lengths, *PtTPX2-1* and *PtTPX2-2*, were comprised of a total of 20/19 exons and 19/18 introns, respectively. The remaining genes generally contained six to nine exons. All 19 *TPX2* proteins contain the *TPX2* domains (Figure 2). In addition, several members have a plant-specific WAND. Among them, *PtMAP20*, *PtMAP20L1*, *PtMAP20L2*, *PtTPX2-1* and *PtTPX2-2* have the *TPX2* domain. All *PtWDL* proteins have *TPX2*-C<sup>KLEEK</sup> domain, except *PtWDL7*,

*PtWDL11* and *PtWDL13*. Only *PtTPX2-1* and *PtTPX2-2* proteins have *TPX2*\_importin domain and Aurora-binding. *PtWDL10*, *PtWDL11*, *PtWDL13* and *PtWDL14* proteins have WAND domain.

To further analyze the functional regions of *PtTPX2* proteins, the conserved motifs were predicted using the MEME program (Supplementary Figure S1). After MEME analysis, fifteen conserved motifs were predicted and named as Motif 1 ~ Motif 15. By analyzing the motif distribution of *PtTPX2* proteins, the C-terminus of all members contained a well-conserved Motif 1. Most subclass members exhibited a common motif composition. Each subclass had different conserved motifs in the N-terminus regions, such as Motif 12 in subclass II, Motif 10 in subclass III, Motif 6 in subclass IV and Motif 3 in subclass VI, indicating that the specific motif was related to specific biological functions.

### 3.3 Analysis of *PtTPX2* proteins' intrinsically disordered regions

The phase separation of proteins is ubiquitous in cell biology. Multiple MAPs contain a substantial percentage of intrinsically disordered regions (IDRs), which can contribute to protein coacervation and phase separation (Pak et al., 2016). Previous studies have shown that the *Xenopus* *TPX2* protein undergoes phase separation to form droplets with tubulin, which is essential for microtubule nucleation (King and Petry, 2020; Safari et al., 2021). Since phase separation often occurs in proteins that have intrinsically disordered regions, we analyzed all *PtTPX2* proteins using PONDR program (designed to predict the protein disordered regions) (Figure 3). All 19 *PtTPX2* proteins were predicted to have disordered regions (average prediction score were greater than 0.5). The *PtMAP20L1*, *PtMAP20L2*, *PtWDL1*, *PtWDL5*, *PtWDL6* and *PtWDL7* proteins were highly disordered among all regions. Particularly, the average prediction score of *PtWDL5* and *PtWDL7* were greater than 0.9. *PtTPX2-1* and *PtTPX2-2* were both highly disordered in the N- and C-termini. The disordered



regions of each protein exhibited high diversity. Based on the above results and the functional reports from previous studies, PtTPX2 proteins may play different biological functions through phase separation under different conditions.

### 3.4 Promoter analysis of PtTPX2 genes

To elucidate the possible regulatory mechanisms of the PtTPX2 genes in abiotic stress responses, we extracted the 2000 bp sequences upstream of the transcription start site to analyze the cis-acting elements (Supplementary Table S3). We listed the cis-acting elements which are related to development-related, hormone responsive, light responsive and stress responsive in Figure 4. Most promoter regions of PtTPX2 genes contained the Myeloblastosis (MYB) and Myelocytomatosis (MYC) binding sites, which are associated with salt and drought stress responses. In addition, we counted the number of developmental, hormonal, light, and stress-related cis-acting elements (Figure 4). CAT-box, ABA-responsive element (ABRE), GT1, and AU-rich element (ARE) were the most abundance cis-acting elements for development, hormone, light, and stress response, respectively. These results indicated that PtTPX2 genes is capable of responding to a wide range of abiotic stresses to perform biological functions.

### 3.5 Chromosome distribution and collinear analysis

The chromosome distribution of the PtTPX2 genes was mapped using the TBtools software based on annotated information on the genome structure of *Populus trichocarpa*, *Arabidopsis thaliana*, *Gossypium hirsutum* and *Eucalyptus grandis*. The 19 PtTPX2 genes were unevenly distributed on 11 chromosomes of *Populus trichocarpa* (Figure 5), indicating the diversification and complexity of the TPX2 family. Chr10 contained four TPX2 genes, three of

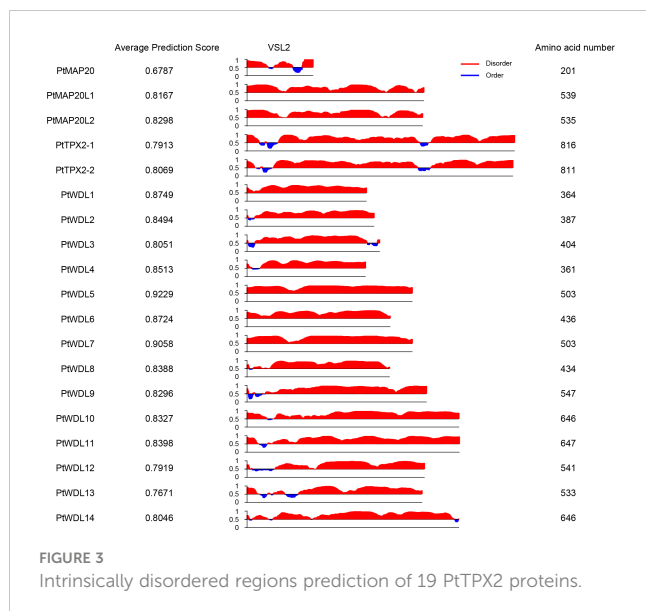
which belonged to Subclass VI. Chr08 and Chr17 both contained three TPX2 genes. Chr06 contained two TPX2 genes, both of which belonged to Subclass V. Chr01, Chr04, Chr05, Chr07, Chr13, Chr16 and Chr18 each contained one TPX2 gene. Gene duplication events were detected by MCScanX, and tandem duplicated genes were not detected. Collinearity analysis showed that all PtTPX2 had at least one collinear gene, except PtWDL9 and PtMAP20 (Figure 5). In order to further analyze the homology and collinearity of TPX2 genes in different species, we also performed an interspecies collinearity analysis using the Multiple Synteny Plot function of TBtools software. A comparison of the collinear genomic blocks of *Populus trichocarpa* with *Arabidopsis thaliana*, *Gossypium hirsutum* and *Eucalyptus grandis*, showed that several PtTPX2 genes were homologous (Figure 6) owing to chromosomal segmental duplication. *Populus trichocarpa* and *Gossypium hirsutum* were more collinear gene pairs. This conclusion suggests that *Populus trichocarpa* was more closely related to *Gossypium hirsutum*. This maybe attributable to that *Populus trichocarpa* and *Gossypium hirsutum* grow in similar environments. These results suggested that segmental duplication was essential in generating of the PtTPX2 genes family in *Populus trichocarpa*.

### 3.6 Expression profiles of PtTPX2 genes in different plant tissues

Tissue-specific expression analysis showed that PtTPX2 gene expression levels were significantly different in different tissues, but almost all PtTPX2 genes had low expression levels in mature leaves, stems and roots (Figure 7; Supplementary Table S4). There was obvious clustering among different subclass members of PtTPX2, and PtMAP20, belonging to the Subclass I, was significantly different from other genes. The expression levels and trends of PtMAP20L1 and PtMAP20L2 in different tissues were basically consistent, they belong to Subclass II. The expression of all PtWDL genes in young leaves was significantly higher than that in other tissues. The expression of PtMAP20 gene showed the highest trend in mature stems, but it was low expressed in young leaves. PtWDL11 also showed high expression in mature leaves, but the expression level was still lower than the young leaves. In addition, PtWDL1 and PtWDL10 were also highly expressed in young stems, but significantly lower than their expression in young leaves. Notably, the expression of PtWDL6 is highly expressed in both young leaves and young stems and the expression level in young stems is higher than that in other tissues, whereas PtWDL5, PtWDL7 and PtWDL8, its closest homolog, were highly expressed only in the young leaves.

### 3.7 Analysis of PtTPX2 genes based on RT-qPCR under salt stress

Under salt stress, PtWDL genes in stems showed an up-regulation phenomenon with the increase of treatment time, except for PtWDL1 and PtWDL12. The expression of PtWDL11, PtWDL12 and PtWDL14 genes showed a decreasing trend in leaves.



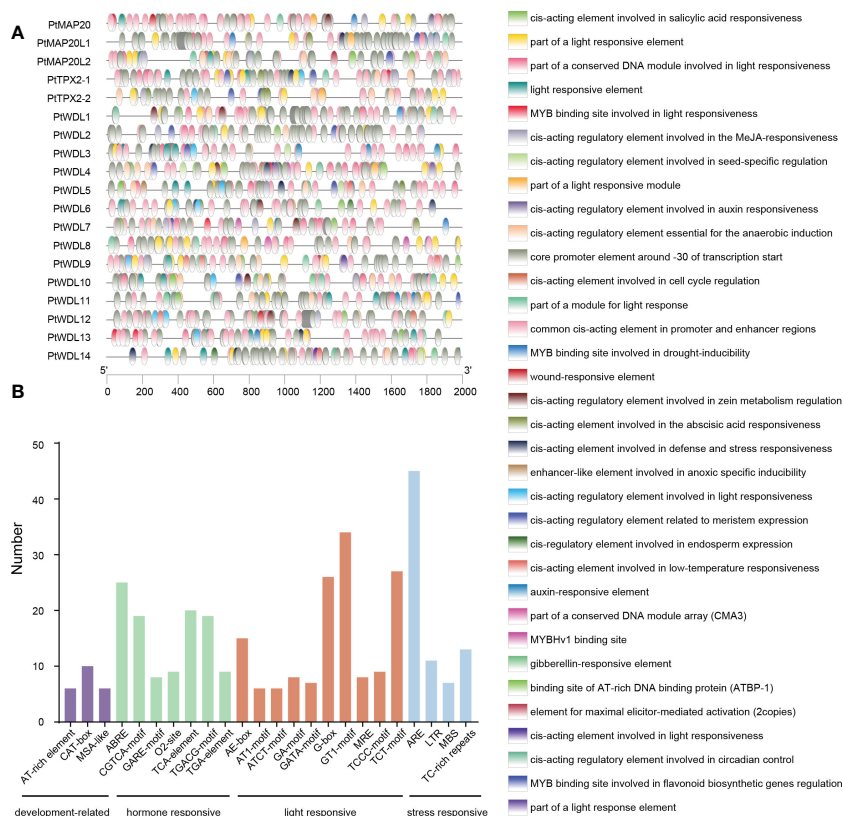
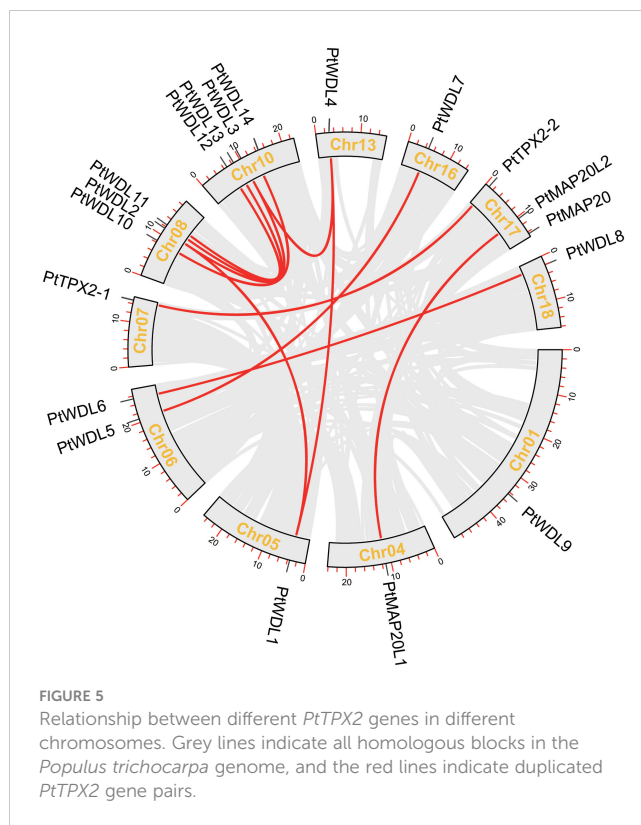


**FIGURE 4** Analysis of *cis*-acting elements in the promoter regions of *PtTPX2* genes. **(A)** Types and distribution locations of *cis*-acting elements in the promoter region of *PtTPX2* gene. **(B)** The number of *cis*-acting elements in the promoter regions of *PtTPX2* genes.

Notably, *PtWDL11*, *PtWDL12* and *PtWDL14* genes all belong to Subclass VI. Moreover, these genes were all expressed without salt stress, suggesting that they may be involved in the regulation of poplar growth. The expressions of *PtMAP20* and *PtMAP20L1* showed an increasing trend in leaves and reached the highest level in 18 h. Additionally, the expressions of *PtMAP20L2*, *PtTPX2-1* and *PtTPX2-2* all increased first and then decreased, the expression levels of them peaked after 12 h of salt stress (Figure 8) (Supplementary Table S4), suggesting that they might have similar functions throughout the salt stress period. The results showed that the expression levels of all *PtWDL* genes increased significantly in the late stage of salt stress, suggesting that they may be more involved in the regulation activities in the late stage of salt stress.

### 3.8 Analysis of *PtTPX2* genes based on RT-qPCR under heat stress

The present study results showed that the expression profiles of *PtTPX2* showed genes different responses to artificially simulated temperature (42°C) stress for different durations. Moreover, the expression profiles of *PtTPX2* also showed significant differences among different tissues. Under heat stress, all *PtTPX2* genes have the most obvious changes in leaves and stems, which indicates that



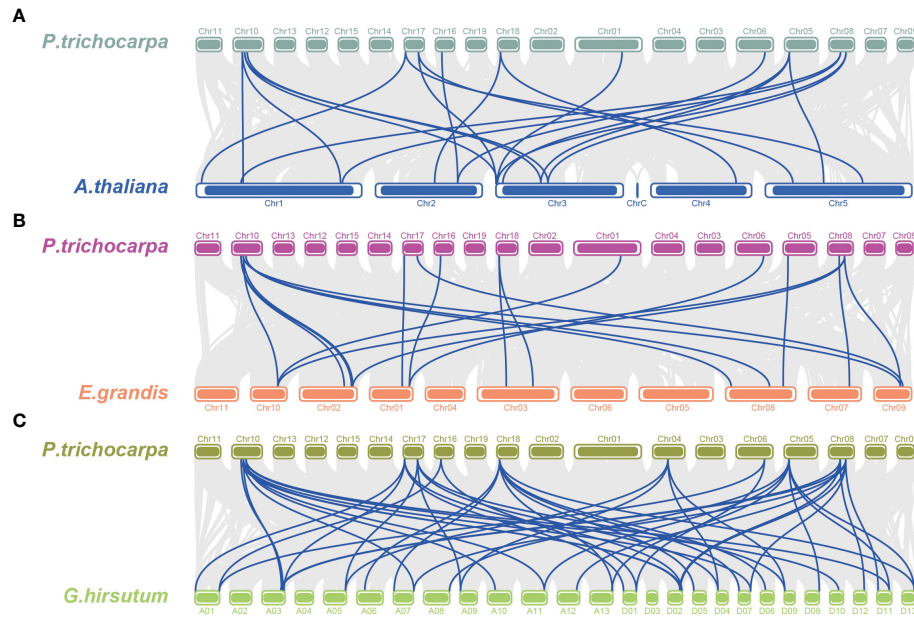


**FIGURE 6**  
Collinearity analysis between different genomes. **(A)** Collinear analysis of *Populus trichocarpa* and *Arabidopsis thaliana*. **(B)** Collinear analysis of *Populus trichocarpa* and *Eucalyptus grandis*. **(C)** Collinear analysis of *Populus trichocarpa* and *Gossypium hirsutum*. Grey lines indicate the collinear blocks within *Populus trichocarpa* and different genomes, the blue line indicates collinear gene pairs.

*PtTPX2* genes directly respond to heat stress and play biological functions in the above-ground parts of the plant. The present study results showed that most of the *PtTPX2* genes had the highest expression at 18 h after heat stress in the stems. However, several genes are different. *PtMAP20*, belong to Subclass I, was peaked in 12 h after heat stress in the stems. *PtTPX2-1* and *PtWDL1* were peaked in 24 h after heat stress in the stems. *PtTPX2-2*, *PtWDL3* and *PtWDL10* were peaked in 24 h after heat stress in the leaves. These results indicate that these genes play a regulatory role in the late stage of heat stress. *PtWDL4*, belong to Subclass IV, was peaked in 6 h after heat stress in the leaves, suggesting that it can play a regulatory role in the early stage of heat stress, which also proves that the leaf organs of plants are crucial for the perception of heat stress. In addition, the expression of *PtWDL8* and *PtWDL12* did not change significantly in stems. *PtWDL8* and *PtWDL12* was highly expressed in roots and leaves without heat stress, but could not be detected after heat stress (Figure 9). These results indicate that *PtTPX2* genes mostly respond to heat stress in the stems.

### 3.9 Analysis of *PtTPX2* genes based on RT-qPCR under drought stress

*PtWDL4*, *PtWDL5* and *PtWDL6*, belong to Subclass IV and V, were up-regulated in leaves, roots and stems tissues over time under drought stress, suggesting that these genes may play a key role in poplar’s specific response to drought stress. Furthermore, *PtMAP20*, *PtMAP20L1* and *PtMAP20L2* were only significantly expressed in stems. The expression of *PtMAP20* and *PtMAP20L1* reached a peak at the 6 h of drought treatment, and then decreased. These results suggest that these genes may play a role in the early stages of drought

stress. However, *PtMAP20L2*, belong to Subclass II with *PtMAP20L1*, was a high expression level without drought stress, suggesting that the growth of poplar itself is regulated by *PtMAP20L2*. Notably, *PtWDL1* and *PtWDL7* may have similar biological functions to *PtMAP20L2*. In addition, the expressions of *PtWDL11*, *PtWDL12*, *PtWDL13* and

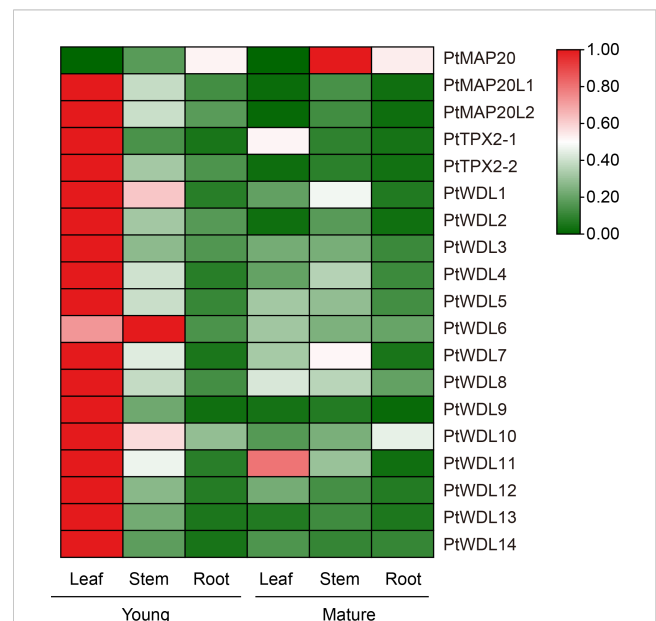


**FIGURE 7**  
Heatmap of *PtTPX2* gene expression patterns in different growing periods, young and mature. Green represents lower gene expression levels and red represents higher gene expression levels. The color represents the level of expression of each gene in each sample. The gene expression levels were calculated based on  $2^{-\Delta\Delta C_t}$ .

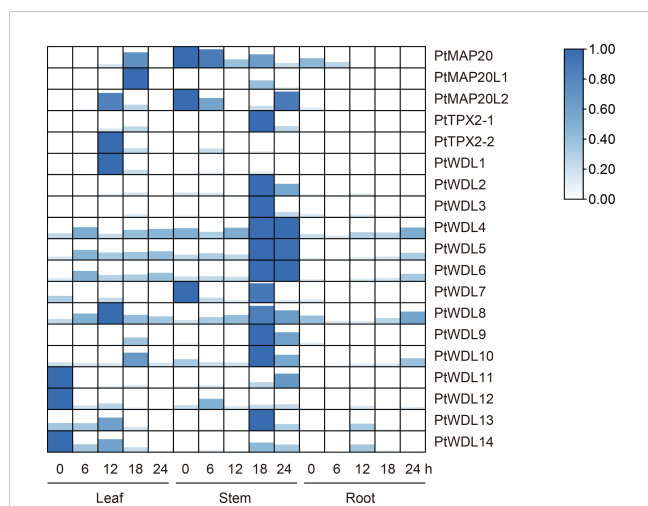


**FIGURE 8**  
Heatmap of *PtTPX2* gene expression patterns in different tissues and processing time under salt stress. The graphic size and color represent the level of expression of each gene in each sample. The gene expression levels were calculated based on  $2^{-\Delta\Delta Ct}$ .

*PtWDL14* were only significantly down-regulated in leaves. Moreover, these genes peaked without drought stress, suggesting that these genes might not be regulated by drought stress (Figure 10). These results suggest that *PtTPX2* genes differently respond to drought stress, however, these genes in the same subclass mostly have similar biological functions.

### 3.10 Subcellular localization analysis of PtWDL6

Based on the above results, *PtWDL6* is significantly respond to salt, drought and heat stresses. Therefore, *PtWDL6* was cloned and

studied in the following work. *PtWDL6*-GFP and MBD-mCherry (labeled MTs) were temporarily expressed in tobacco leaf epidermal cells and visualized by a confocal laser-scanning microscope (Figure 11). As shown in Figure 11, the *PtWDL6*-GFP fluorescence overlapped with the red fluorescent signal of cortical MTs. Colocalization was analyzed by plotting the signal intensities of *PtWDL6*-GFP and MTs using ImageJ software (Figure 11). As demonstrated, *PtWDL6* localized to MTs in the tobacco cells.

## 4 Discussion

The microtubule is a dynamic and adaptive structure, and its functions and dynamics depend on regulation by microtubule-associated proteins (Dixit and Cyr, 2004; Ehrhardt and Shaw, 2006; Akhmanova and Steinmetz, 2010; Hamant et al., 2019). TPX2 is a class of conserved microtubule-associated proteins which regulate microtubule dynamics in response to diverse developmental and environmental cues (Wittmann et al., 2000; Neumayer et al., 2014; Wadsworth, 2015). Poplar has a high economic value and serves as a model for elucidating molecular mechanisms of development and stress tolerance in tree species. However, genome-wide analyses of the *TPX2* genes of *Populus trichocarpa* have not been performed, and the regulatory functions of *PtTPX2* genes involved in abiotic stress responses remain unclear. In the present study, 19 *PtTPX2* genes were screened and systematically analyzed. The phylogenetic analysis was conducted with four plants species: *Populus trichocarpa*, *Eucalyptus grandis*, *Gossypium hirsutum* and *Arabidopsis thaliana*. The TPX2 protein family in *Populus trichocarpa* was divided into six subclasses to further identifying the protein conservation. The similar arrangements of gene structures and conserved motifs in the same subclass further prove the correctness of the *TPX2* classifications. All *TPX2* members contained well-conserved motif

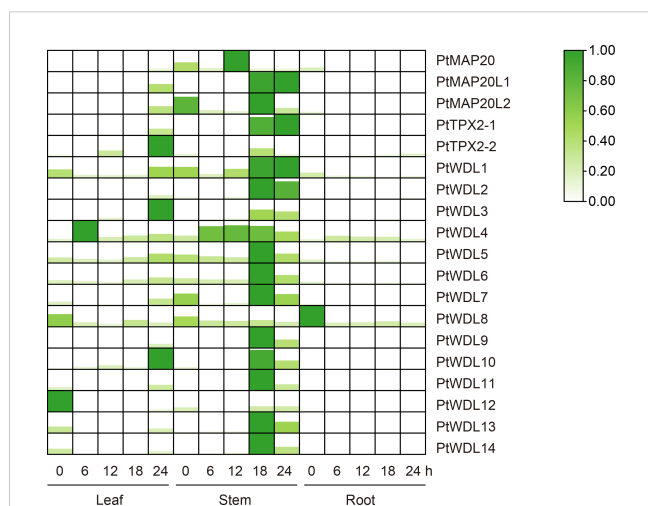


**FIGURE 9**  
Heatmap of *PtTPX2* gene expression patterns in different tissues and processing time under heat stress. The graphic size and color represent the level of expression of each gene in each sample. The gene expression levels were calculated based on  $2^{-\Delta\Delta Ct}$ .

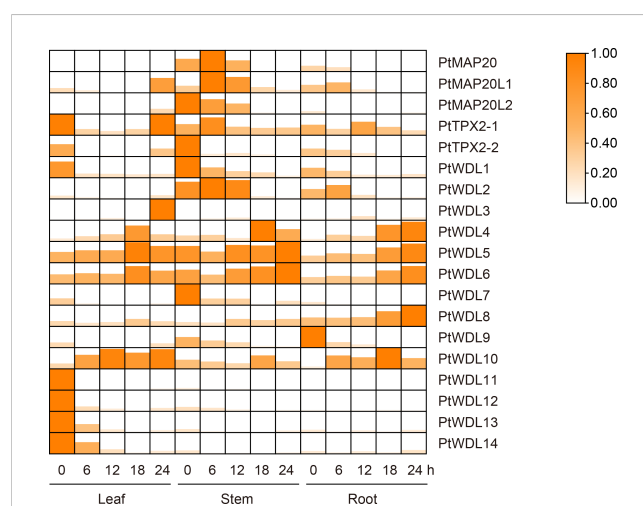


**FIGURE 10**  
Heatmap of *PtTPX2* gene expression patterns in different tissues and processing time under drought stress. The graphic size and color represent the level of expression of each gene in each sample. The gene expression levels were calculated based on  $2^{-\Delta\Delta Ct}$ .

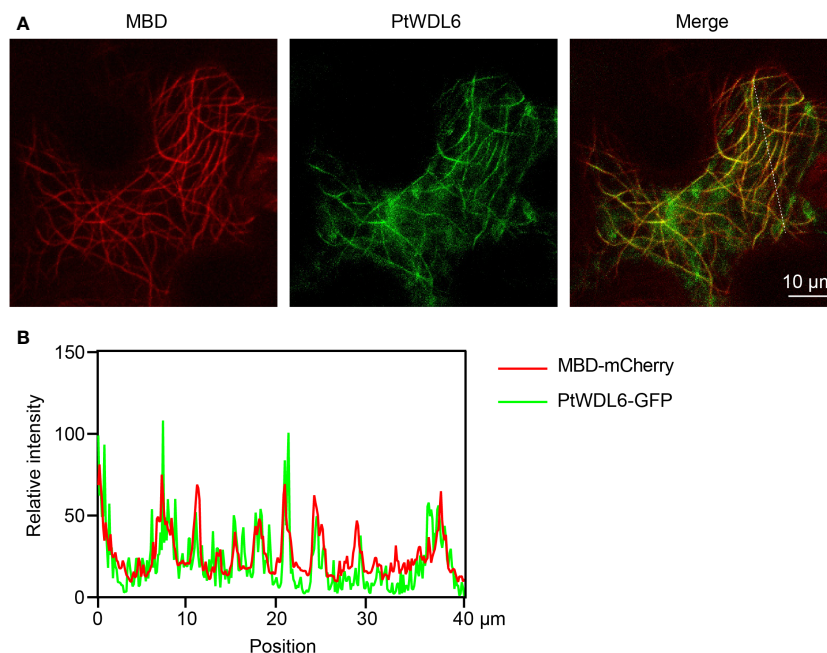


FIGURE 11

Subcellular localization of PtWDL6 proteins. (A) PtWDL6 colocalizes with cortical MTs detected in tobacco cells. (B) Plot of a line scan drawn showing a strong correlation between the spatial localization of PtWDL6 and cortical MTs.

1 in the C-terminus regions, and subclass members had different conserved motifs in the N-terminus regions, suggesting that *TPX2* genes may have different biological functions.

Under abiotic stresses, plants usually activate various mechanisms to resist the adverse environment (Chai et al., 2016). Soil salinization is one of the main factors affecting the productivity of forestry (Yang et al., 2018; Litalien and Zeeb, 2020; Van Zelm et al., 2020). Under high-salinity conditions, excessive cytosolic  $\text{Na}^+$  breaks the dynamic balance of basic mineral nutrients that limit the growth and development of trees. In addition, multiple studies have demonstrated that many other regulatory factors and molecular mechanisms are involved in the process by which plants resist salt stress (Osakabe et al., 2014; Zhao et al., 2018; Wei et al., 2022; Deng et al., 2023). Heat stress is one of the important ecological factors affecting plant physiological processes. In recent years, with the impact of climate change such as the increase in global average temperature, the phenomenon of plants suffering from heat stress has become more and more frequent (Hassan et al., 2021). Plants respond to heat stress mainly through the activation of subsequent molecular cascades associated with heat shock factors and their main targets (heat shock proteins), to cellular responses and then to the plant's own phenotypic response against heat stress (Kang et al., 2022). Drought stress seriously affects plant growth, development, reproduction and other life activities. It also affects plant morphology, structure and physiological function. Changes in plant biomass, water use efficiency, photosynthetic system, osmotic regulation ability, cell membrane stability, antioxidant system defense ability and hormone levels are often used to judge

the ability of plants to resist drought stress (Kuromori et al., 2022). In this study, *PtTPX2* gene was differentially expressed in response to salt, heat and drought stresses. In addition, *TPX2* genes in different plant tissues were also responsive to cold and osmotic stresses (Kumar et al., 2016).

The microtubule cytoskeleton controls plant growth and cell morphogenesis, as well as participates in the adaptation of plants to stress. Cortical MTs reorganized new microtubule networks to aid plant survival under stress. Several MAPs have been implicated in these processes (Wang et al., 2011; Zhang et al., 2012; Li et al., 2017). Previous studies have shown that some upstream transcription factors regulate the expression of the *AtTPX2* gene (Sun et al., 2015; Dou et al., 2018). Therefore, analyzing the promoter region of genes is conducive to screening candidate upstream regulatory factors. In this study, numerous *cis*-acting elements were found in promoters, and they are closely associated with various abiotic stresses. The promoter region of *PtTPX2* contained a large number of binding elements, which are also related to the stress response (Major et al., 2017; Guo et al., 2022). The results of RT-qPCR showed that salt stress, heat stress and drought stress can significantly change the *PtTPX2* gene in different tissues or treatment times. This indicated that *PtTPX2* gene had a positive response to stress treatment (Figure 8–10). In addition, subcellular localization showed that *PtWDL6* was co-localized with MTs in plant cells (Figure 11). That is, *PtWDL6* may respond to abiotic stress by regulating MTs. Therefore, *TPX2* gene may be involved in the regulation of MTs to help plants resist abiotic stresses and adapt to the environment.

## 5 Conclusions

Collectively, 19 *Populus trichocarpa* *TPX2* genes were comprehensively analyzed, including gene structures, phylogenetic characteristics, intrinsically disordered regions, *cis*-regulatory elements, expression patterns and functional characterizations. Through RT-qPCR data mining, we found that *PtTPX2* gene was significantly differentially expressed under various abiotic stresses. Meanwhile, *PtWDL6* was cloned and co-localized with cortical MTs in tobacco cells. Taken together, these findings provide important information for the elucidation of the function of *PtTPX2* genes and establish a foundation for future studies on the role of *TPX2* genes in stress tolerance.

## Data availability statement

The original contributions presented in this study are included in the article/Supplementary Materials. Further inquiries can be directed to the corresponding author.

## Author contributions

NLian conceived and designed the study. NLian, MQ, SW and NLi conducted the experiments and wrote the manuscript. MQ and NLi analyzed the data. SW and LL assisted with the experiments. LL, YZ and JX provided guidance on experimental methods. JW provided the analysis method used for the experimental process. RW revised the manuscript. All authors contributed to the article and approved the submitted version.

## Funding

This research was funded by the Fundamental Research Funds for the Central Universities (BLX202117), and the National Natural Science Foundation of China (32201519).

## References

- Akhmanova, A., and Steinmetz, M. O. (2010). Microtubule+ TIPs at a glance. *J. Cell Sci.* 123, 3415–3419. doi: 10.1242/jcs.062414
- Bailey, T. L., and Gribskov, M. (1998). Methods and statistics for combining motif match scores. *J. Comput. Biol.* 5, 211–221. doi: 10.1089/cmb.1998.5.211
- Brunet, S., Sardon, T., Zimmerman, T., Wittmann, T., Pepperkok, R., Karsenti, E., et al. (2004). Characterization of the TPX2 domains involved in microtubule nucleation and spindle assembly in xenopus egg extracts. *Mol. Biol. Cell* 15, 5318–5328. doi: 10.1091/mbc.e04-05-0385
- Cao, H., Amin, R., Niu, L., Song, Z., Dong, B., Li, H., et al. (2020). Multidimensional analysis of actin depolymerising factor family in pigeon pea under different environmental stress revealed specific response genes in each subgroup. *Funct. Plant Biol.* 48, 180–194. doi: 10.1071/FP20190
- Chai, Q., Gan, Y., Zhao, C., Xu, H.-L., Waskom, R. M., Niu, Y., et al. (2016). Regulated deficit irrigation for crop production under drought stress. *A review. Agron. Sustain. Dev.* 36, 1–21. doi: 10.1007/s13593-015-0338-6
- Chen, C., Chen, H., Zhang, Y., Thomas, H. R., Frank, M. H., He, Y., et al. (2020). TBtools: an integrative toolkit developed for interactive analyses of big biological data. *Mol. Plant* 13, 1194–1202. doi: 10.1016/j.molp.2020.06.009
- Chen, X., Wu, S., Liu, Z., and Friml, J. (2016). Environmental and endogenous control of cortical microtubule orientation. *Trends Cell Biol.* 26, 409–419. doi: 10.1016/j.tcb.2016.02.003
- Chenna, R., Sugawara, H., Koike, T., Lopez, R., Gibson, T. J., Higgins, D. G., et al. (2003). Multiple sequence alignment with the clustal series of programs. *Nucleic Acids Res.* 31, 3497–3500. doi: 10.1093/nar/gkg500
- Deng, H., Li, Q., Cao, R., Ren, Y., Wang, G., Guo, H., et al. (2023). Overexpression of SmMYC2 enhances salt resistance in arabidopsis thaliana and salvia miltiorrhiza hairy roots. *J. Plant Physiol.* 280, 153862. doi: 10.1016/j.jplph.2022.153862
- Desjardins, P., and Conklin, D. (2010). NanoDrop microvolume quantitation of nucleic acids. *J. Vis. Exp.* 45, e2565. doi: 10.3791/2565
- Dixit, R., and Cyr, R. (2004). The cortical microtubule array: from dynamics to organization. *Plant Cell* 16, 2546–2552. doi: 10.1105/tpc.104.161030

## Conflict of interest

The authors declare that the research was conducted in the absence of any commercial or financial relationships that could be construed as a potential conflict of interest.

## Publisher's note

All claims expressed in this article are solely those of the authors and do not necessarily represent those of their affiliated organizations, or those of the publisher, the editors and the reviewers. Any product that may be evaluated in this article, or claim that may be made by its manufacturer, is not guaranteed or endorsed by the publisher.

## Supplementary material

The Supplementary Material for this article can be found online at: <https://www.frontiersin.org/articles/10.3389/fpls.2023.1159181/full#supplementary-material>

### SUPPLEMENTARY FIGURE 1

Structure of *PtTPX2* genes and motif composition of *PtTPX2* proteins. (UTR: Untranslated Regions. CDS: Coding DNA Sequence).

### SUPPLEMENTARY TABLE 1

qPCR Primers.

### SUPPLEMENTARY TABLE 2

Analysis of the location of *TPX2* in the chromosome.

### SUPPLEMENTARY TABLE 3

Promoter *cis*-acting element analysis.

### SUPPLEMENTARY TABLE 4

*PtTPX2* gene expression patterns.

- Dou, L., He, K., Higaki, T., Wang, X., and Mao, T. (2018). Ethylene signaling modulates cortical microtubule reassembly in response to salt stress. *Plant Physiol.* 176, 2071–2081. doi: 10.1104/pp.17.01124
- Dou, L., He, K., Peng, J., Wang, X., and Mao, T. (2021). The E3 ligase MREL57 modulates microtubule stability and stomatal closure in response to ABA. *Nat. Commun.* 12, 1–15. doi: 10.1038/s41467-021-22455-y
- Ehrhardt, D. W., and Shaw, S. L. (2006). Microtubule dynamics and organization in the plant cortical array. *Annu. Rev. Plant Biol.* 57, 859–875. doi: 10.1146/annurev.arplant.57.032905.105329
- Fletcher, D. A., and Mullins, R. D. (2010). Cell mechanics and the cytoskeleton. *Nature* 463, 485–492. doi: 10.1038/nature08908
- Guo, Q., Major, I. T., Kapali, G., and Howe, G. A. (2022). MYC transcription factors coordinate tryptophan-dependent defence responses and compromise seed yield in arabidopsis. *New Phytol.* 236, 132–145. doi: 10.1111/nph.18293
- Hamada, T. (2014). Microtubule organization and microtubule-associated proteins in plant cells. *Int. Rev. Cell Mol. Biol.* 312, 1–52. doi: 10.1016/B978-0-12-800178-3.00001-4
- Hamant, O., Inoue, D., Bouchez, D., Dumais, J., and Mjolsness, E. (2019). Are microtubules tension sensors? *Nat. Commun.* 10, 1–12. doi: 10.1038/s41467-019-10207-y
- Hassan, M. U., Chattha, M. U., Khan, I., Chattha, M. B., Barbanti, L., Aamer, M., et al. (2021). Heat stress in cultivated plants: Nature, impact, mechanisms, and mitigation strategies—a review. *Plant Biosystems-An Int. J. Dealing all Aspects Plant Biol.* 155, 211–234. doi: 10.1080/11263504.2020.1727987
- Kang, Y., Lee, K., Hoshikawa, K., Kang, M., and Jang, S. (2022). Molecular bases of heat stress responses in vegetable crops with focusing on heat shock factors and heat shock proteins. *Front. Plant Sci.* 13, 837152. doi: 10.3389/fpls.2022.837152
- King, M. R., and Petry, S. (2020). Phase separation of TPX2 enhances and spatially coordinates microtubule nucleation. *Nat. Commun.* 11, 1–13. doi: 10.1038/s41467-019-14087-0
- Kumar, D., Hazra, S., Datta, R., and Chattopadhyay, S. (2016). Transcriptome analysis of arabidopsis mutants suggests a crosstalk between ABA, ethylene and GSH against combined cold and osmotic stress. *Sci. Rep.* 6, 36867. doi: 10.1038/srep36867
- Kuromori, T., Fujita, M., Takahashi, F., Yamaguchi-Shinozaki, K., and Shinozaki, K. (2022). Inter-tissue and inter-organ signaling in drought stress response and phenotyping of drought tolerance. *Plant Journal: Cell Mol. Biol.* 109, 342–358. doi: 10.1111/tpj.15619
- Lei, K., Liu, A., Fan, S., Peng, H., Zou, X., Zhen, Z., et al. (2019). Identification of TPX2 gene family in upland cotton and its functional analysis in cotton fiber development. *Genes* 10, 508. doi: 10.3390/genes10070508
- Lescot, M., Déhais, P., Thijs, G., Marchal, K., Moreau, Y., Van de Peer, Y., et al. (2002). PlantCARE, a database of plant cis-acting regulatory elements and a portal to tools for in silico analysis of promoter sequences. *Nucleic Acids Res.* 30, 325–327. doi: 10.1093/nar/30.1.325
- Li, C., Lu, H., Li, W., Yuan, M., and Fu, Y. (2017). A ROP2-RIC1 pathway fine-tunes microtubule reorganization for salt tolerance in arabidopsis. *Plant Cell Environ.* 40, 1127–1142. doi: 10.1111/pce.12905
- Lian, N., Liu, X., Wang, X., Zhou, Y., Li, H., Li, J., et al. (2017). COP1 mediates dark-specific degradation of microtubule-associated protein WDL3 in regulating arabidopsis hypocotyl elongation. *Proc. Natl. Acad. Sci.* 114, 12321–12326. doi: 10.1073/pnas.1708087114
- Lian, N., Wang, X., Jing, Y., and Lin, J. (2021). Regulation of cytoskeleton-associated protein activities: Linking cellular signals to plant cytoskeletal function. *J. Integr. Plant Biol.* 63, 241–250. doi: 10.1111/jipb.13046
- Litalien, A., and Zeeb, B. (2020). Curing the earth: A review of anthropogenic soil salinization and plant-based strategies for sustainable mitigation. *Sci. Total Environ.* 698, 134235. doi: 10.1016/j.scitotenv.2019.134235
- Liu, X., Qin, T., Ma, Q., Sun, J., Liu, Z., Yuan, M., et al. (2013). Light-regulated hypocotyl elongation involves proteasome-dependent degradation of the microtubule regulatory protein WDL3 in arabidopsis. *Plant Cell* 25, 1740–1755. doi: 10.1105/tpc.113.112789
- Lloyd, C. (2011). Dynamic microtubules and the texture of plant cell walls. *Int. Rev. Cell Mol. Biol.* 287, 287–329. doi: 10.1016/B978-0-12-386043-9.00007-4
- Luo, W., Xiao, N., Wu, F., Mo, B., Kong, W., and Yu, Y. (2022). Genome-wide identification and characterization of YUCCA gene family in *mikania micrantha*. *Int. J. Mol. Sci.* 23, 13037. doi: 10.3390/ijms232113037
- Major, I. T., Yoshida, Y., Campos, M. L., Kapali, G., Xin, X. F., Sugimoto, K., et al. (2017). Regulation of growth–defense balance by the JASMONATE ZIM-DOMAIN (JAZ)-MYC transcriptional module. *New Phytol.* 215, 1533–1547. doi: 10.1111/nph.14638
- Meng, D., Li, Y., Bai, Y., Li, M., and Cheng, L. (2016). Genome-wide identification and characterization of WRKY transcriptional factor family in apple and analysis of their responses to waterlogging and drought stress. *Plant Physiol. Biochem.* 103, 71–83. doi: 10.1016/j.plaphy.2016.02.006
- Neumayer, G., Belzil, C., Gruss, O. J., and Nguyen, M. D. (2014). TPX2: of spindle assembly, DNA damage response, and cancer. *Cell. Mol. Life Sci.* 71, 3027–3047. doi: 10.1007/s00018-014-1582-7
- Osakabe, Y., Yamaguchi-Shinozaki, K., Shinozaki, K., and Tran, L. S. P. (2014). ABA control of plant macroelement membrane transport systems in response to water deficit and high salinity. *New Phytol.* 202, 35–49. doi: 10.1111/nph.12613
- Pak, C. W., Kosno, M., Holehouse, A. S., Padrick, S. B., Mittal, A., Ali, R., et al. (2016). Sequence determinants of intracellular phase separation by complex coacervation of a disordered protein. *Mol. Cell* 63, 72–85. doi: 10.1016/j.molcel.2016.05.042
- Perrin, R. M., Wang, Y., Yuen, C. Y., Will, J., and Masson, P. H. (2007). WVD2 is a novel microtubule-associated protein in arabidopsis thaliana. *Plant J.* 49, 961–971. doi: 10.1111/j.1365-313X.2006.03015.x
- Qi, M., Wu, R., Song, Z., Dong, B., Chen, T., Wang, M., et al. (2022). Sorbitol reduces sensitivity to alternaria by promoting ceramide kinases (CERK) expression through transcription factor Pswrky25 in populus (*Populus simonii* carr.). *Genes* 13, 405. doi: 10.3390/genes13030405
- Rajangam, A. S., Kumar, M., Aspeborg, H., Guerriero, G., Arvestad, L., Pansri, P., et al. (2008). MAP20, a microtubule-associated protein in the secondary cell walls of hybrid aspen, is a target of the cellulose synthesis inhibitor 2, 6-dichlorobenzonitrile. *Plant Physiol.* 148, 1283–1294. doi: 10.1104/pp.108.121913
- Ren, H., Dang, X., Cai, X., Yu, P., Li, Y., Zhang, S., et al. (2017). Spatio-temporal orientation of microtubules controls conical cell shape in arabidopsis thaliana petals. *PLoS Genet.* 13, e1006851. doi: 10.1371/journal.pgen.1006851
- Safari, M. S., King, M. R., Brangwynne, C. P., and Petry, S. (2021). Interaction of spindle assembly factor TPX2 with importins- $\alpha/\beta$  inhibits protein phase separation. *J. Biol. Chem.* 297 (3), 100998. doi: 10.1016/j.jbc.2021.100998
- Smertenko, A., Clare, S. J., Effertz, K., Parish, A., Ross, A., and Schmidt, S. (2021). A guide to plant TPX2-like and WAVE-DAMPENED2-like proteins. *J. Exp. Bot.* 72, 1034–1045. doi: 10.1093/jxb/eraa513
- Smertenko, T., Turner, G., Fahy, D., Brew-Appiah, R. A., Alfaro-Aco, R., de Almeida Engler, J., et al. (2020). Brachypodium distachyon MAP20 functions in metaxylem pit development and contributes to drought recovery. *New Phytol.* 227, 1681–1695. doi: 10.1111/nph.16383
- Sun, J., Ma, Q., and Mao, T. (2015). Ethylene regulates the arabidopsis microtubule-associated protein WAVE-DAMPENED2-LIKE5 in etiolated hypocotyl elongation. *Plant Physiol.* 169, 325–337. doi: 10.1104/pp.15.00609
- Tuskan, G. A., Difazio, S., Jansson, S., Bohlmann, J., Grigoriev, I., Hellsten, U., et al. (2006). The genome of black cottonwood, populus trichocarpa (Torr. & Gray). *Science* 313, 1596–1604. doi: 10.1126/science.1128691
- Van Zelm, E., Zhang, Y., and Testerink, C. (2020). Salt tolerance mechanisms of plants. *Annu. Rev. Plant Biol.* 71, 403–433. doi: 10.1146/annurev-arplant-050718-100005
- Voorrips, R. (2002). MapChart: software for the graphical presentation of linkage maps and QTLs. *J. heredit.* 93, 77–78. doi: 10.1093/jhered/93.1.77
- Vos, J. W., Pieuchot, L., Evrard, J.-L., Janski, N., Bergdoll, M., de Ronde, D., et al. (2008). The plant TPX2 protein regulates proteasome assembly before nuclear envelope breakdown. *Plant Cell* 20, 2783–2797. doi: 10.1105/tpc.107.056796
- Wadsworth, P. (2015). Tpx2. *Curr. Biol.* 25, R1156–R1158. doi: 10.1016/j.cub.2015.10.003
- Wang, S., Kurepa, J., Hashimoto, T., and Smalle, J. A. (2011). Salt stress-induced disassembly of arabidopsis cortical microtubule arrays involves 26S proteasome-dependent degradation of SPIRAL1. *Plant Cell* 23, 3412–3427. doi: 10.1105/tpc.111.089920
- Wang, X., and Mao, T. (2019). Understanding the functions and mechanisms of plant cytoskeleton in response to environmental signals. *Curr. Opin. Plant Biol.* 52, 86–96. doi: 10.1016/j.pbi.2019.08.002
- Wang, C., Zhang, L., and Chen, W. (2011). Plant cortical microtubules are putative sensors under abiotic stresses. *Biochem. (Moscow)* 76, 320–326. doi: 10.1134/S0006297911030047
- Wei, X., Fan, X., Zhang, H., Jiao, P., Jiang, Z., Lu, X., et al. (2022). Overexpression of ZmSRG7 improves drought and salt tolerance in maize (*Zea mays* L.). *Int. J. Mol. Sci.* 23, 13349. doi: 10.3390/ijms232113349
- Wittmann, T., Wilm, M., Karsenti, E., and Vernos, I. (2000). TPX2, a novel xenopus MAP involved in spindle pole organization. *J. Cell Biol.* 149, 1405–1418. doi: 10.1083/jcb.149.7.1405
- Wu, Y., Chang, L., Jiang, C., Xu, L., and Zhang, J. (2021). “Plastid transformation in poplar: A model for perennial trees,” in *Chloroplast biotechnology* (New York, NY: Springer US), pp 257–pp 265.
- Xu, M., Chen, C., Cai, H., and Wu, L. (2018). Overexpression of PeHKT1; 1 improves salt tolerance in populus. *Genes* 9, 475. doi: 10.3390/genes9100475
- Xue, B., Dunbrack, R. L., Williams, R. W., Dunker, A. K., and Uversky, V. N. (2010). PONDR-FIT: a meta-predictor of intrinsically disordered amino acids. *Biochim. Biophys. Acta (BBA)-Proteins Proteomics* 1804, 996–1010. doi: 10.1016/j.bbapap.2010.01.011
- Yang, L., Wen, K.-S., Ruan, X., Zhao, Y.-X., Wei, F., and Wang, Q. (2018). Response of plant secondary metabolites to environmental factors. *Molecules* 23, 762. doi: 10.3390/molecules23040762
- Zhang, Q., Lin, F., Mao, T., Nie, J., Yan, M., Yuan, M., et al. (2012). Phosphatidic acid regulates microtubule organization by interacting with MAP65-1 in response to salt stress in arabidopsis. *Plant Cell* 24, 4555–4576. doi: 10.1105/tpc.112.104182
- Zhang, X., Liu, L., Chen, B., Qin, Z., Xiao, Y., Zhang, Y., et al. (2019). Progress in understanding the physiological and molecular responses of populus to salt stress. *Int. J. Mol. Sci.* 20, 1312. doi: 10.3390/ijms20061312
- Zhao, C., Zayed, O., Yu, Z., Jiang, W., Zhu, P., Hsu, C.-C., et al. (2018). Leucine-rich repeat extensin proteins regulate plant salt tolerance in arabidopsis. *Proc. Natl. Acad. Sci.* 115, 13123–13128. doi: 10.1073/pnas.1816991115